haematologica
Journal of the Ferrata Storti Foundation

Expanded clinical, genetic and biological spectrum of filaminopathies with hematological involvement

by Charlotte Brillon, Marjorie Poggi, Mathieu Fiore, Cyril Goizet, Sophie Bayart, Melanie Y. Daniel, Jean-Baptiste Valentin, Nathalie Hezard, Johannes Van Agthoven, Veronique Sbarra, Marie Loosveld, Céline Falaise, Marie-Christine Alessi, Manal Ibrahim-Kosta and Paul Saultier

Received: June 17, 2025.
Accepted: October 1, 2025.

Citation: Charlotte Brillon, Marjorie Poggi, Mathieu Fiore, Cyril Goizet, Sophie Bayart, Melanie Y. Daniel, Jean-Baptiste Valentin, Nathalie Hezard, Johannes Van Agthoven, Veronique Sbarra, Marie Loosveld, Céline Falaise, Marie-Christine Alessi, Manal Ibrahim-Kosta and Paul Saultier. Expanded clinical, genetic and biological spectrum of filaminopathies with hematological involvement. Haematologica. 2025 Oct 9. doi: 10.3324/haematol.2025.288445 [Epub ahead of print]

Expanded clinical, genetic, and biological spectrum of filaminopathies with hematological involvement.

Charlotte Brillon[1], Marjorie Poggi[2], Mathieu Fiore[3], Cyril Goizet[4], Sophie Bayart[5], Mélanie Y. Daniel[6], Jean-Baptiste Valentin[7], Nathalie Hezard[8], Johannes Van Agthoven[9], Véronique Sbarra[2], Marie Loosveld[8], Céline Falaise[1], Marie-Christine Alessi[10], Manal Ibrahim-Kosta[10], Paul Saultier[1].

[1]Department of Pediatric Hematology, Immunology and Oncology, Aix Marseille University, APHM, INSERM, INRAE, C2VN, La Timone Children's Hospital, Marseille, France.
[2]Aix-Marseille University, INSERM, INRAE, C2VN, Marseille, France.
[3]Department of Hematology, Reference Center for Inherited Platelet Disorders, University of Bordeaux, University Hospital of Bordeaux, INSERM, U1034, Pessac, France.
[4]Department of Genetics, Reference Center for Neurogenetics, University Hospital of Bordeaux, Bordeaux, France.
[5]Reference Center for Hemophila and other Coagulation Factors Deficiency, Reference Center for Inherited Platelet Disorders and von Willebrand's Disease, University Hospital of Rennes, France.
[6]Hematology and Transfusion Department, French National Institute for Health and Medical Research, University Hospital of Lille, Pasteur Institute of Lille, University of Lille, U1011 - European Genomic Institute for Diabetes, Lille, France.
[7]Hemophilia Treatment Center, University Hospital of Tours, Tours, France.
[8]Hematology Laboratory, CHU Timone, Marseille, France.
[9]Structural Biology Program, Division of Nephrology/Department of Medicine, Massachusetts General Hospital and Harvard Medical School, Charlestown, MA, USA.
[10]Hematology Laboratory, Reference Center for Inherited Platelet Disorders, Aix-Marseille University, APHM, INSERM, INRAE, C2VN, Marseille, France.

Author contributions : M.F., S.B, C.G., M.Y, J.-B.V., N.H., C.F., M.I.-K., M.L. and M.-C.A. performed the clinical and biological characterization of patients. V.S. and M.P.

performed the functional experiments. P.S., M.I.-K., M.P. and M.-C.A. conceived and supervised the project. J.V.-A. performed the structural analysis of the protein. C.B. and P.S. analyzed the data and wrote the manuscript.

Running heads: Filaminopathy A: hematological insight.

Corresponding author: Marjorie Poggi, C2VN, Faculté de Médecine, Aix-Marseille University, 27 Boulevard Jean Moulin, 13385 Marseille, France.
Email: marjorie.poggi@univ-amu.fr

Data-sharing statement: the dataset generated and analyzed are available from the corresponding author on request.

Disclosure: there are no competing interests to disclose.

Word count: 1653 words. 2 figures and 1 table.
Supplementary files: 3 figures and 1 table.

Trial registration: ClinicalTrials.gov identifier: NCT04419987 - EVGPP: study of the functionality of new genetic variants at the origin of constitutional platelet pathologies, Application Number: 2019-A03054-53.

Funding: the authors declare no sources of fundings.

Main Text:

Constitutional thrombocytopenias represent a heterogeneous group of rare diseases where thrombocytopenia can signal complex, multi-organ disorder. One example is filaminopathy A, a very rare and probably underdiagnosed disease[1] that accounts for approximately 1% of inherited thrombocytopenia (unpublished data from the French reference center for inherited platelet disorders [CRPP]). It is caused by variants in the *Filamin A (FLNA)* gene. This gene, located on the X-chromosome, encodes a ubiquitous actin-binding protein interacting with over 90 partners involved in intracellular signaling and cytoskeletal reorganization.[2] Among its many roles, FLNA is known to interact with proteins involved in platelet production and activation, such as αIIbβ3 (GPIIb/IIIa) and GPIb, supporting its role in thrombopoiesis and platelet functions.[2] Thrombocytopenia is a recognized but variably penetrant manifestation. A recent literature review regrouping 170 patients carrying pathogenic *FLNA* variants reported platelet abnormalities in 11 individuals, although hematological data were missing for most cases, suggesting potential underreporting.[3] A classical feature occurs in females carrying a null *FLNA* variant responsible for a loss-of-function of the protein. These patients typically present with periventricular nodular heterotopia (PNH), seizures, Ehlers-Danlos-like connective tissue symptoms, and macrothrombocytopenia. Several teams have shown that females harboring a null variant have two platelet subpopulations, one lacking FLNA.[4] In hemizygous males, null *FLNA* variants can cause severe or fatal perinatal manifestations.[5] In contrast, the pathogenicity of missense variants remains debated. Some have been reported as potentially pathogenic, but apart from those affecting the first 150 amino acids (exon 2) and impairing FLNA-actin binding, little is known about how others affect platelet phenotype and the underlying mechanisms.[5–7] Thus, classifying missense *FLNA* variants in thrombocytopenic patients with suspected milder filaminopathies is challenging.

This study retrospectively collected clinical and biological data from patients referred to the CRPP with *FLNA* variants. It aimed to describe a large cohort of patients with *FLNA* variants and hematological involvement and identify indicators suggesting filaminopathy as the underlying cause of thrombocytopenia. Flow cytometry measurement (FCM) and immunofluorescence (IF) were used to assess intraplatelet FLNA in patients and controls. Sixteen *FLNA* variants were studied in eighteen

patients, including two relatives (Figure 1A). All cases were included after informed consent in accordance with the Declaration of Helsinki. Variants were identified using a gene panel sequencing for platelet disorders, as previously described.[8] This is the largest cohort to date focusing on hematological manifestations of filaminopathy A. Patients were categorized according to the type of *FLNA* variants. The first group, with a null variant, had a classical phenotype, including PNH as a discriminating feature, along with cardiac and vascular defects, hyperlaxity, and gastrointestinal and pulmonary disorders. All had FLNA-negative platelets. The second group had missense variants, absent or rare in general population databases, with computational evidence of deleterious effects on the protein. They had a subtler phenotype, lacked FLNA-negative platelets, and sometimes had an alternative diagnosis explaining their thrombocytopenia.

Ten variants were classified as null (12 patients), including three nonsense, five frameshift, one high splice variant (c.2404+1del; patient 11, P11), and one large duplication of exons 2-29. All were classified as pathogenic according to the American College of Medical Genetics (ACMG) guidelines (Table S1)[9].

Patients carrying null variants displayed the classical filaminopathy phenotype (Table 1). Cardiac and vascular defects were common (n=9/12), including valvular malformations, persistent ductus arteriosus (PDA), aortic aneurysms, and venous insufficiency. Digestive disorders (n=3/12), such as malrotation and chronic intestinal pseudo-obstruction (CIPO), along with respiratory disorders (n=2/12), including emphysema and severe asthma, were also observed. Two patients reported hyperlaxity. Neurological features were prominent. Brain magnetic resonance imaging (MRI) was performed in all but P9, although she had seizures. MRI revealed PNH in ten patients, a hallmark of filaminopathy, as other causes are anecdotal.[4] P12 had a distinctive neurological profile. This male patient, carrying a large *FLNA* duplication, exhibited brain MRI abnormalities (severe demyelination, hydrocephaly) but no PNH or neurological symptoms. Seven patients had epilepsy, and four experienced learning disabilities or mood disorders. This highlights the importance of brain MRI in suspected *FLNA*-related thrombocytopenia, even in asymptomatic cases.

From a hematological perspective, all patients had mild to moderate thrombocytopenia (50–150 G/L), with three exhibiting large or giant platelets (Figure S1). Hemorrhagic manifestations were predominantly mucocutaneous, particularly easy bruising and abnormal uterine bleeding, as well as provoked bleeding during hemostatic challenges (mainly postpartum hemorrhage). Evaluation using the international society on thrombosis and hemostasis bleeding assessment tool (ISTH-BAT) indicated mild bleeding symptoms in most cases, with scores generally below or near the established diagnostic thresholds (≥4 for males, ≥6 for females and ≥3 for children).[10] These findings corroborate the previous reports,[4,11] although hematologic aspects were often overlooked, making this the largest study of *FLNA* variants associated with bleeding disorders.

Intra-platelet FLNA was assessed in six patients using FCM (n=6) and IF (n=1) (Figure 2). Among female patients, two distinct platelet subpopulations were identified: FLNA-positive and FLNA-negative, with FLNA-negative platelets ranging from 25% to 75%. A proportion below 50% suggests shorter half-life of FLNA-positive platelets.[11] Two patients exhibited FLNA-negative platelets exceeding 50%, possibly due to variable X chromosome inactivation. P12, the only male of the cohort carrying a null variant (exon 2-29 duplication), displayed exclusively FLNA-negative platelets, consistent with full impairment of his single *FLNA* allele. Despite a typical phenotype (mild macrothrombocytopenia, CIPO, PDA, aortic aneurysm), P12 lacked epilepsy and PNH on MRI, but showed microbleeds, demyelination, and ventricular dilatations, reflecting the heterogeneous presentation of filaminopathy A,[12] particularly in males with potential mosaicism.[13] Therefore, screening for filaminopathy is recommended for males. FCM findings align with IF data (Figure 2B), supporting prior IF studies.[4,6,14] Both FCM and IF confirmed that FLNA-negative platelets are larger than FLNA-positive ones (Figure S2). FLNA-deficient megakaryocytes prematurely release large, fragile platelets.[11] By providing quantitative data, FCM constitutes a valuable approach for diagnosing thrombocytopenia caused by *FLNA* null variants. It also provides a functional method for classifying intronic splicing variants. Intraplatelet quantification may serve as an early screening tool for constitutional thrombocytopenia, supporting filaminopathy diagnosis before genetic confirmation or clinical complications arise.

The other six variants were missense and classified as variants of “uncertain significance” (class 3 using ACMG guidelines). Predicted deleterious by multiple bioinformatics tools, they were absent or rare in general population databases (GnomAD) (Table S1). They affected nucleotides conserved across species (human, mouse, zebrafish, drosophila), with three located in highly conserved regions (Figure 1B).

Patients carrying missense variants had mild to moderate thrombocytopenia (50–120 G/L) or even a normal platelet count (P13). Large or giant platelets were observed in two patients (Figure S1).

Their overall clinical picture was complex (Table 1), including bleeding manifestations (n=4/6), cardiac malformations (n=2/6), lung disorders (n=2/6), hyperlaxity (n=1/6), and autoimmune disorders. Notably, no seizures or PNH were observed, although only three patients underwent brain MRI. Several PNH cases with a missense *FLNA* variant have been reported,[15] but data on the variants' pathogenicity and platelet count were lacking.

Intra-platelet FLNA study using FCM (n=5) and IF (n=5) showed no FLNA-negative platelets (Figure 2), suggesting thrombocytopenia might result from qualitative rather than quantitative FLNA defect, or may even be independent of FLNA. Further functional assays are needed to elucidate the impact of these missense variants.

In P15 and P16, genetic analyses identified alternative molecular etiologies for their hematological phenotype. P15 had a genetically confirmed telomeropathy (two heterozygous “likely pathogenic” variants in *TERT*, p.Ser12Phe, and p.Phe560Leu). P16 had an *ACTN1*-related thrombocytopenia (“likely pathogenic” variant p.Arg738Gln).[14] Although these alternative genetic causes satisfy BP5 criteria from the ACMG guidelines, they are insufficient to reclassify *FLNA* variants as “likely benign”. However, they suggest that the *FLNA* variant is unlikely to be the primary cause of thrombocytopenia in these cases. P13, the only patient in the cohort with a normal platelet count, despite mucocutaneous hemorrhage and provoked bleeding, had no alternative molecular diagnosis. However functional platelet studies revealed a dense granule deficiency, potentially explaining the bleeding tendency. P17 carried an *ACTN1* variant of “uncertain significance” (p.Ala587Val), which could explain the disease as plausibly as the *FLNA* variant. Genetic investigations and routine

functional studies did not identify any other etiology for thrombocytopenia in P14 and P18.

Structural studies provided further insights. Cryo-electron microscopy of the actin-binding domain complex showed binding within the calponin-homology 1 (CH1) domain (Lys43-Ser149).[17] Variant P13 (p.Arg190Trp) in CH2 (Gln166-Leu269), lies outside actin-binding sequences, supporting the alternative diagnosis of dense granule deficiency. Variant P14 (p.Gly452Ser) and P16 (p.Thr1685ala), may impact the protein's folding (protein stability free energy change (ΔΔG) -0.179 and -0.069 kcal/mol, respectively), possibly affecting its stability. In contrast, P17 (p.His2124Gln), had a slight stabilizing effect (ΔΔG 0.044 kcal/mol). This variant lies within the GPIbα-binding domain, deletion of which has shown no significant impact on proplatelet formation in vitro.[18] Variant P15 (p.Ala1252Val) affects Ig-like domain 11 in a loop connecting it to Ig-10, without clear structural implication, supporting the alternative diagnosis of telomeropathy. Variant P18 (p.Arg2264Glu) is near the β3 C-terminal binding site of αIIbβ3 integrin (Figure S3). Modeling within conformer 16 of the Ig21-αIIbβ3 C-terminal complex NMR structure showed a disruptive ΔΔG of 1.01 kcal/mol. This variant may weaken FLNA-αIIbβ3 interaction, which appears to play a crucial role in RhoA pathway downregulation,[18] thereby affecting actomyosin contractility and proplatelet formation.

This study reports the clinical, genetic, and biological characteristics of the largest cohort of filaminopathies A with hematological involvement. It highlights the importance of considering the type of *FLNA* variant and its association with specific clinical features. Thrombocytopenia is typically mild, large and giant platelets may be observed, and platelet function testing reveals non-specific or even normal findings, making the platelet phenotype insufficiently distinctive in its own. The presence of PNH on brain MRI and FLNA-negative platelets are strong indicators of *FLNA*-related thrombocytopenia and may constitute an effective screening method for diagnosis as suggested by previous reports[4,14,19,20]. The causal role of missense variation was ruled out in three out of the six cases indicating that, in absence of PNH, caution should be exercised when interpreting this type of variation. Further research is needed to better understand the contribution of missense variants to *FLNA*-related thrombocytopenia.

References

1. Chen MH, Walsh CA. FLNA Deficiency. In: Adam MP, Feldman J, Mirzaa GM, Pagon RA, Wallace SE, Bean LJ et al., editors. GeneReviews® [Internet]. Seattle (WA): University of Washington, Seattle; 1993-. 2021 Sep 30. Available from: https://www.ncbi.nlm.nih.gov/sites/books/NBK1213/ Accessed on 2025, Aug 6.

2. Rosa J-P, Raslova H, Bryckaert M. Filamin A: key actor in platelet biology. Blood. 2019;134(16):1279-1288.

3. Vassallo P, Westbury SK, Mumford AD. FLNA variants associated with disorders of platelet number or function. Platelets. 2020;31(8):1097-1100.

4. Ieda D, Hori I, Nakamura Y, et al. A novel truncating mutation in FLNA causes periventricular nodular heterotopia, Ehlers-Danlos-like collagenopathy and macrothrombocytopenia. Brain Dev. 2018;40(6):489-492.

5. Loft Nagel J, Jønch AE, Nguyen NTTN, Bygum A. Phenotypic manifestations in FLNA-related periventricular nodular heterotopia: a case report and review of the literature. BMJ Case Rep. 2022;15(4):e247268.

6. Berrou E, Adam F, Lebret M, et al. Heterogeneity of platelet functional alterations in patients with filamin A mutations. Arterioscler Thromb Vasc Biol. 2013;33(1):e11-18.

7. Kunishima S, Ito-Yamamura Y, Hayakawa A, Yamamoto T, Saito H. FLNA p.V528M substitution is neither associated with bilateral periventricular nodular heterotopia nor with macrothrombocytopenia. J Hum Genet. 2010;55(12):844-846.

8. Saultier P, Vidal L, Canault M, et al. Macrothrombocytopenia and dense granule deficiency associated with FLI1 variants: ultrastructural and pathogenic features. Haematologica. 2017;102(6):1006-1016.

9. Richards S, Aziz N, Bale S, et al. Standards and Guidelines for the Interpretation of Sequence Variants: A Joint Consensus Recommendation of the American College of Medical Genetics and Genomics and the Association for Molecular Pathology. Genet Med. 2015;17(5):405-424.

10. Elbatarny M, Mollah S, Grabell J, et al. Normal range of bleeding scores for the ISTH-BAT: adult and pediatric data from the merging project. Haemophilia. 2014;20(6):831-835.

11. Jurak Begonja A, Hoffmeister KM, Hartwig JH, Falet H. FlnA-null megakaryocytes prematurely release large and fragile platelets that circulate poorly. Blood. 2011;118(8):2285-2295.

12. Sheen VL, Dixon PH, Fox JW, et al. Mutations in the X-linked filamin 1 gene cause periventricular nodular heterotopia in males as well as in females. Hum Mol Genet. 2001;10(17):1775-1783.

13. Oegema R, Hulst JM, Theuns-Valks SDM, et al. Novel no-stop FLNA mutation causes multi-organ involvement in males. Am J Med Genet. A 2013;161A(9):2376-2384.

14. Tanner LM, Kunishima S, Lehtinen E, et al. Platelet function and filamin A expression in two families with novel FLNA gene mutations associated with periventricular nodular heterotopia and panlobular emphysema. Am J Med Genet A. 2022;188(6):1716-1722.

15. Yang L, Wu G, Yin H, Pan M, Zhu Y. Periventricular nodular heterotopias is associated with mutation at the FLNA locus-a case history and a literature review. BMC Pediatr. 2023;23(1):346.

16. Boutroux H, David B, Guéguen P, et al. ACTN1-related Macrothrombocytopenia: A Novel Entity in the Progressing Field of Pediatric Thrombocytopenia. J Pediatr Hematol Oncol. 2017;39(8):e515-e518.

17. Iwamoto DV, Huehn A, Simon B, et al. Structural basis of the filamin A actin-binding domain interaction with F-actin. Nat Struct Mol Biol. 2018;25(10):918-927.

18. Donada A, Balayn N, Sliwa D, et al. Disrupted filamin A/αIIbβ3 interaction induces macrothrombocytopenia by increasing RhoA activity. Blood. 2019;133(16):1778-1788.

19. Zaninetti C, Leinøe E, Lozano ML, et al. Validation of immunofluorescence analysis of blood smears in patients with inherited platelet disorders. J Thromb Haemost. 2023;21(4):1010-1019.

20. Greinacher A, Pecci A, Kunishima S, et al. Diagnosis of inherited platelet disorders on a blood smear: a tool to facilitate worldwide diagnosis of platelet disorders. J Thromb Haemost. 2017;15(7):1511-1521.

21. Noris P, Biino G, Pecci A, et al. Platelet diameters in inherited thrombocytopenias: analysis of 376 patients with all known disorders. Blood. 2014;124(6):e4-e10.

		Age at diagnosis	Hematological manifestations				Neurological manifestations		Cardiovascular manifestations	Other		
		/	Platelet count ($x10^9$/L) mean [range]	Large / Giant platelets**	Platelet dysfunction ***	ISTH-BAT score****	Brain MRI	Clinical manifestations	/	Pulmonary involvement	Gastro-intestinal mani-festations	Other
Null variants*	**P1 (F)** c.133C>T	29	111 [110-130]	10% / 2%	No	6	PNH	Epilepsy Learning disabilities Mood disorders	Bicuspid aortic valve Mitral dysplasia	0	0	Spinal anomalies Retro-auricular fistula Alopecia
	P2 (F) c.133C>T	31	71 [50-80]	A few / 0%	Yes	1	PNH	Epilepsy Learning disabilities Mood disorders	Patent ductus arteriosus Aortic regurgitation Dilated ascending aorta Varicous vein	0	Common mesentery	Retro-auricular fistula
	P3 (F) c.639G>A	48	99 [97-104]	NA	NA	NA	PNH	0	Patent ductus arteriosus	0	0	0
	P4 (F) c.1056delG	42	118 [106-125]	0% / 0%	Yes	4	PNH	Epilepsy	Aortic regurgitation Dilated ascending aorta Varicous vein	0	0	Hyperlaxity Raynaud Hashimoto Strabism
	P5 (F) c.1056delG	8	120 [114-130]	10% / 4%	Yes	1	PNH	Epilepsy Learning disabilities Mood disorders	Dysplastic aortic valve Aortic regurgitation	0	Chronic interstitial gastritis	Hyperlaxity Strabism
	P6 (F) c.1120_1125 delinsTCTTG	24	149 [133-169]	5% / 0%	No	3	PNH	Epilepsy Learning disabilities Mood disorders	Atrial and ventricular septal defects Mitral and aortic regurgitations Dilated ascending aorta	Emphysema Obstructive ventilatory defect	0	Hyperlaxity
	P7 (F) c.1835C>A	7	156 [148-165]	0% / 0%	No	3	PNH	0	Dilated aorta	0	0	0
	P8 (F) c.3677_3684 del	NA	144	NA	NA	NA	PNH	0	Dilated aorta	0	0	0
	P9 (F) c.5027_5030 del	22	134	NA	Yes	2	NA	Epilepsy	0	Emphysema Severe asthma Pneumo-thorax	0	0
	P10 (F) c.5146dup	55	119 [116-122]	8% / 3%	Yes	3	PNH	Epilepsy	NA	NA	0	0
	P11 (F) c.2404+1del	37	114 [102-129]	0% / 0%	Yes	2	PNH	0	NA	NA	0	0
	P12 (M) Duplication of exons 2 to 29	14	95 [60-125]	A few / 0%	No	2	Demyelination Ventricular dilatations	0	Patent ductus arteriosus Aortic aneurysm Dissection of the iliac artery	0	CIPO	Abnormal erythrocytes morphology
Missense variants*	**P13 (F)** c.568C>T	44	266 [232-295]	3% / 0%	Yes	10	Normal	0	Mitral and aortic regurgitations	0	0	Miscarriages

P14 (F) c.1354G>A	30	134 [124-152]	3% / 0%	No	6	Normal	0	0	Asthma	0	0
P15 (F) c.3755C>T	13	31 [22-78]	A few / 0%	No	3	NA	0	0	Restrictive ventilatory defect Lung diffusion impairment	Hepatopathy	Hyperlaxity Anti-thyroid antibodies Pancytopenia
P16 (F) c.5053A>G	21	141 [130-162]	12% / 1%	Yes	4	NA	NA	NA	0	0	0
P17 (F) c.6372C>G	32	98	4% / 0%	No	0	NA	NA	0	0	0	Miscarriages
P18 (M) c.6791G>A	13	60	50% / 2%	No	2	Normal	NA	Left ventricular compaction	0	0	Dental agenesis

*All null variants were classified as ACMG class 5, and all missense variants as ACMG class 3.

** Large platelets are defined as platelets with a diameter equal or larger than half the diameter of an erythrocyte and giant platelet are defined as platelets with a diameter equal or larger than the size of an erythrocyte. The proportions of large and giant platelets are <10% and <1% in healthy individuals, respectively.[21]

***Light transmission aggregometry was performed in P1, P2, P4, P5, P6, P7, P11, P12, P13, P14, P15, P16, P17 and P18. TME was performed in P13. PFA-100 was performed in P1, P2, P11 and P17. Quantification of intraplatelet serotonin was performed in P1, P2, P4, P5, P6, P9, P13, P14, P15 and P16. Mepacrine uptake and release assay was performed in P1, P2, P4, P5, P7, P9, P10, P11, P13, P14, P15 and P16. Platelet granule release assay was performed in P7 and P10. Flow cytometry analysis of platelet membrane glycoproteins was performed in P1, P2, P4, P5, P7, P11, P12, P13, P14, P15, P16 and P18. Intraplatelet plasminogen activator inhibitor-1 (PAI-1) quantification was performed in P1, P2, P4, P5, P6, P9 and P16.

****The international society on thrombosis and hemostasis – bleeding assessment tool (ISTH-BAT) score at diagnosis was obtained either by retrospectively calculating it from bleeding histories documented in patient records or by directly using scores previously assessed and recorded by the hematologists managing the patients. The accepted normal score ranges vary according to sex and age: 0–3 for males, 0–5 for females, and 0–2 for children.

Table 1: Clinical and biological features of the 18 patients included in the analysis. Clinical and biological data were retrospectively collected from patients referred to the French reference center of hereditary platelet disorders who were found to have either a null or a missense *FLNA* variant using a high-throughput sequencing panel targeting genes associated with constitutional platelet diseases. Patients P1 to P12 (light grey) have null *FLNA* variants, while patients P13 to P18 (dark grey) have missense *FLNA* variants. PNH was assessed using MRI. F = female / M = male / MRI = magnetic resonance imaging / PNH = nodular periventricular heterotopia / MPV = mean platelet volume / ADP = adenosine diphosphate / TRAP = thrombin receptor activator peptide / NA = not available / CIPO = chronic intestinal pseudo-obstruction

Figure legends

Figure 1: Filamin A (FLNA) protein structure and variants analysis. (A) Domains of the protein and studied variants of the cohort. FLNA is a large dimeric actin-binding protein, each monomer consisting of 2646 amino acids (280 kDa). Its structure consists of two calponin homology sequences forming the actin binding domain in the N-terminal, followed by 24 immunoglobulin-like (Ig-like) domain repeats (90-100 amino acids). Rod 1 domain is a linear arrangement of Ig 1 to 15 separated from Rod 2 domain by Hinge 1. Rod 2 is more compact as it is made up of Ig 16 to 23 working in pairs. This part of the protein contains most of the binding sites, leading to numerous interactions with different partners. It ends with Hinge 2 followed by Ig24, which represents the C-terminal part of the protein and allows the dimerization. The null *FLNA* variants are written in blue, the missense variants are written in dark. **(B) Sequence alignment.** The amino-acid sequence of human FLNA protein was compared to orthologs using Clustal OMEGA (http://www.ebi.ac.uk/Tools/msa/clustalo/). The missense variants reported in this study alter the residues Arg190, Gly452, Ala1252, Thr1685, His2124 and Arg2264. The table gives the corresponding residue in three other species (mouse, zebrafish and drosophila).

Figure 2: Evaluation of intraplatelet Filamin A. (A) Quantification of intraplatelet FLNA with flow cytometry measurement. Whole blood samples (100 µL) anticoagulated with ethylenediaminetetraacetic acid (EDTA) were initially fixed using paraformaldehyde to a final concentration of 1% (vol/vol) for 10 minutes. Subsequently, centrifugation at 1000g for 5 minutes at room temperature was performed. The cell pellet was then resuspended in a permeabilization buffer consisting of PBS with 2 mM EDTA, 0.5% BSA, and 0.5% Triton X-100 to ensure adequate permeabilization. On the following day, 10 µL of the fixed and permeabilized cells were stained for 15 minutes with antibodies against CD41 (CD41 APC, BD 559777 clone HIP8) and FLNA (C-ter) (FLNa A488, ab246749, epitope located within the final 100 amino acids of the protein) at room temperature. Finally, 200 µL of PBS was added to the samples prior to FCM analysis to evaluate the expression of the target proteins. Upper panel: representative cytometric analysis of a control subject and two patients, one carrying a missense variant (P17,

p.His2124Gln) and one carrying a null variant (P4, p.Thr353LeufsTer32). Lower panel: the boxplots represent the percentage of FLNA-negative platelets obtained with FCM for the control group (n=13), the patients carrying a missense variant (n=5) and those carrying a null variant (n=6). All patients with a null variant exhibited FLNA-negative platelets, ranging from 25% to 100%. In contrast, all platelets from the control subjects and from patients with a missense variant expressed FLNA. **(B) Evaluation of intraplatelet FLNA with immunofluorescence.** Fluorescence microscopy analysis comparing the distribution of FLNA and von Willebrand Factor (VWF) in fixed cells from 6 patients and 1 healthy control. Cells were fixed with pre-cooled methanol for one minute at -20°C and washed three times with Phosphate Buffered Saline (PBS) containing 0.5% Bovine Serum Albumin (BSA). A 30-minute incubation with PBS:0.5% BSA was undertaken as a blocking procedure. The primary antibodies, mouse anti-filamin A (sc-71118, 1:50) and rabbit anti-VWF (Dako, 1:500), were incubated at room temperature for one to two hours, followed by three PBS washes. Secondary antibodies, anti-mouse Alexa Fluor 488 (A11029, *Invitrogen*, 1:500) and anti-rabbit Alexa Fluor 546 (A11010, *Invitrogen*, 1:500), were subsequently applied, and cells were incubated in a light-free environment. Following a further three washes in PBS, the samples were mounted with Fluoromount containing 4',6-diamidino-2-phenylindole (DAPI) for analysis via fluorescence microscopy. Merged panel: P6 (c.1120_1125delinsTCTTG – p.Val374SerfsTer2) showed 2 subtypes of platelets : FLNA-negative large platelet and FLNA-positive normal size platelet. Note that P18 (c.6791G>A – p.Arg2264Gln) presented FLNA-positive large platelets.

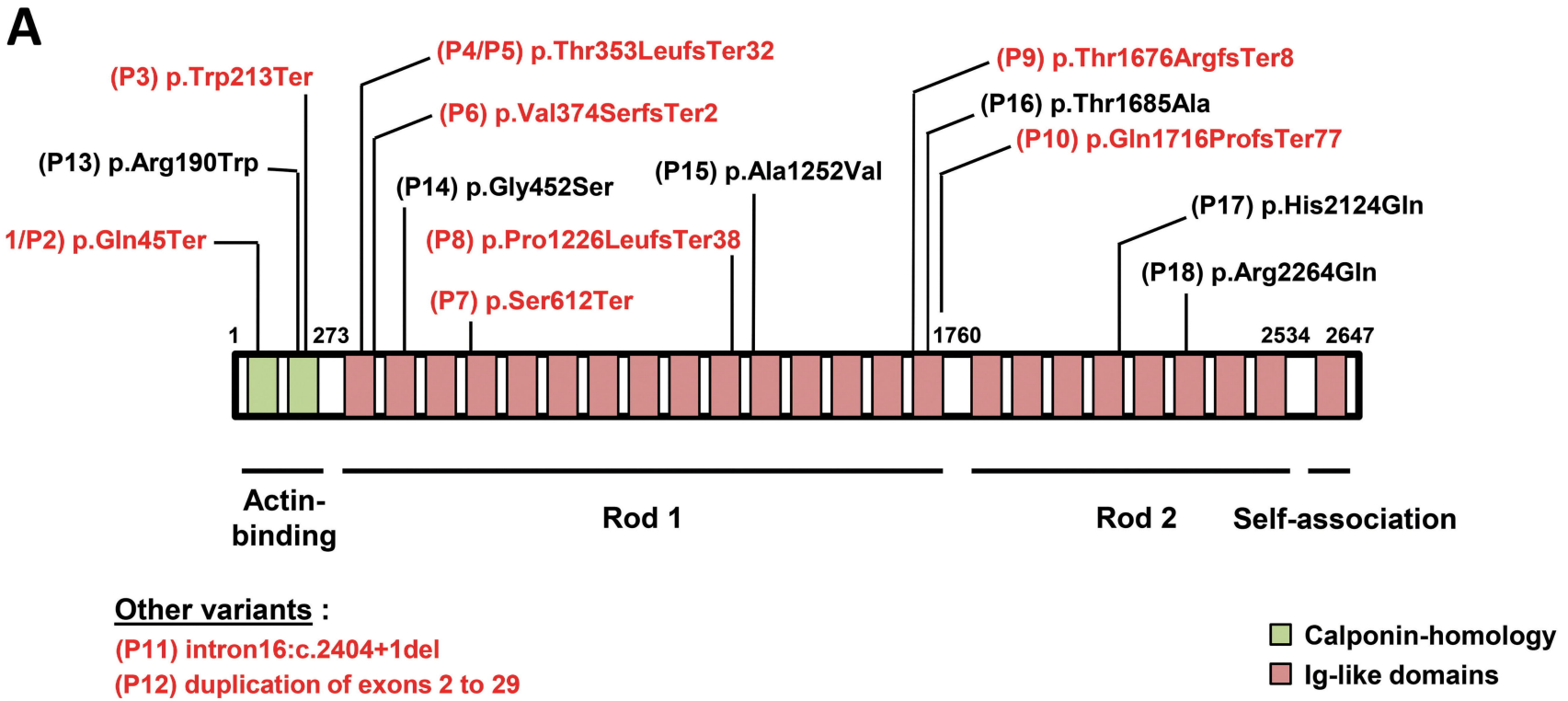

B

```
FLNA R190W      PITNFSWDWQSGR •
FLNA G452S                    • YQPTMESVHTVHV
FLNA A1252V                   •               • KLQVEPVVDTSGV
FLNA T1685A                   •               •               • AGKGKVACTVCTP
FLNA H2116Q                   •               •               •               • IKFADQQVPGSPF •
FLNA R2264Q                   •               •               •               •               • EFSIWTQEAGAGG
Human           PITNFSRDWQSGR • YQPTMEGVHTVHV • KLQVEPAVDTSGV • AGKGKVTCTVCTP • IKFADQHVPGSPF • EFSIWTREAGAGG
Mouse           PITNFSRDWQSGR • YQPTMEGVHTVHV • KLQVEPAVDTSGV • AGKGKVTCTVCTP • IKFADQHVPGSPF • EFGIWTREAGAGG
Zebrafish       PITNFSRDWQSGR • YKPTQEGQHIIYI • RLHVEPAVETSGV • AGKGKVTCTVCTP • VKYQGQHVPGSPF • EFSIWTREAGAGG
Drosophila      PINNFTNDWTTGK • YVTALQGLHSVNV • VKVEGHAGDASKV • AGDGAVTCKITNK • IRFADKHIPGSPF • EFNVWTREAGGGS
```

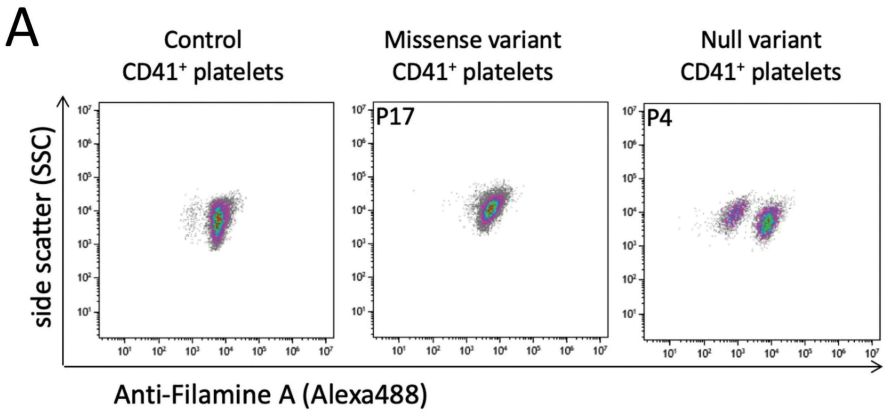
A
Control
CD41+ platelets
Missense variant
CD41+ platelets
Null variant
CD41+ platelets
P17
P4
side scatter (SSC)
Anti-Filamine A (Alexa488)

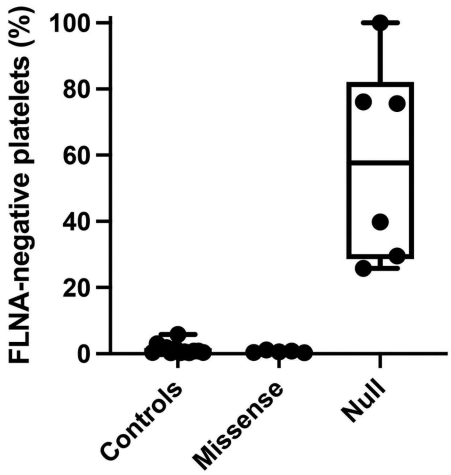
FLNA-negative platelets (%)
100
80
60
40
20
0
Controls
Missense
Null

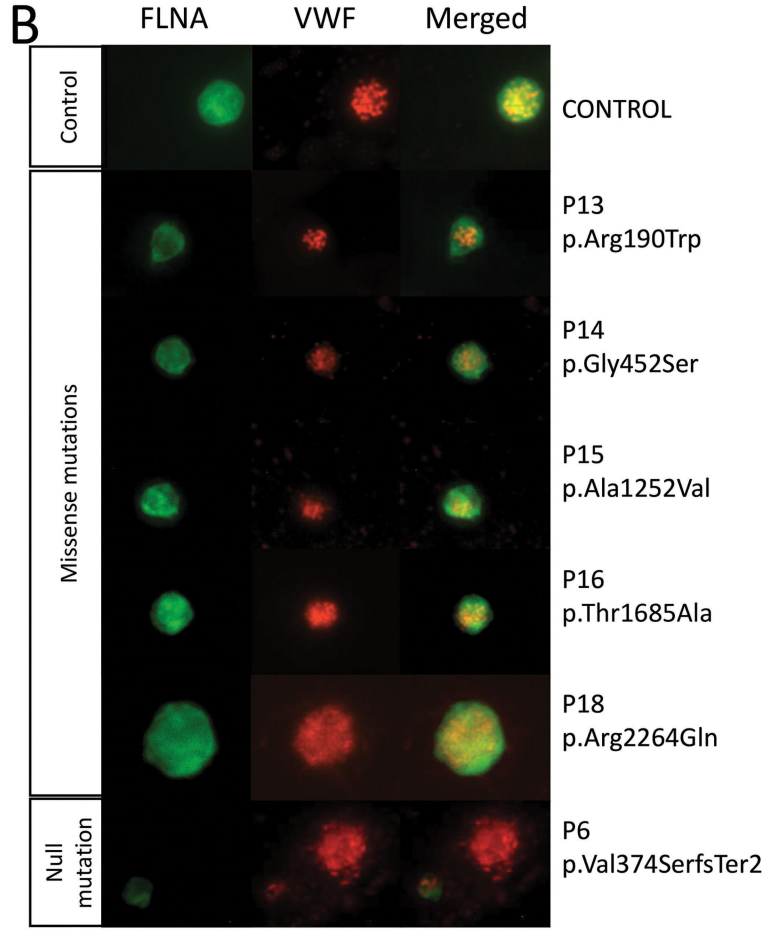
B
FLNA
VWF
Merged
Control
Missense mutations
Null mutation
CONTROL
P13
p.Arg190Trp
P14
p.Gly452Ser
P15
p.Ala1252Val
P16
p.Thr1685Ala
P18
p.Arg2264Gln
P6
p.Val374SerfsTer2

Supplemental Table

Table S1: Genetic characteristics and prediction of pathogenicity for both null and missense *FLNA* variants.

	Patient	Variant DNA	Variant protein	gnomAD exome v.4 frequency	CADD score	ACMG	MPA score
Null variants	**P1** **P2**	exon2:c.133C>T	p.Gln45Ter	*	37	5	10 (nonsense)
	P3	exon 4: c.639G>A	p.Trp213Ter	*	36	5	10 (nonsense)
	P4 **P5**	exon7:c.1056delG	p.Thr353LeufsTer32	*	*	5	10 (frameshift)
	P6	exon8:c.1120_1125delinsTCTTG	p.Val374SerfsTer2	*	*	5	10 (frameshift)
	P7	exon13:c.1835C>A	p.Ser612Ter	*	39	5	10 (nonsense)
	P8	exon22:c.3677_3684del	p.Pro1226LeufsTer38	*	*	5	10 (frameshift)
	P9	exon31:c.5027_5030del	p.Thr1676ArgfsTer8	*	*	5	10 (frameshift)
	P10	exon31:c.5146dup	p.Gln1716ProfsTer77	*	*	5	10 (frameshift)
	P11	intron16:c.2404+1del		*	*	5	10 (high splice)
	P12	Duplication of exons 2 to 29				5	
Missense variants	**P13**	exon3:c.568C>T	p.Arg190Trp	$2.7x10^{-6}$	23	3	9 (high missense)
	P14	exon9:c.1354G>A	p.Gly452Ser	$9.1x10^{-7}$	25	3	10 (high missense)
	P15	exon22:c.3755C>T	p.Ala1252Val	$2.6x10^{-5}$	24	3	9 (high missense)
	P16	exon31 :c.5053A>G	p.Thr1685Ala	*	24	3	10 (high missense)
	P17	exon39 :c.6372C>G	p.His2124Gln	$9.1x10^{-7}$	24	3	10 (high missense)
	P18	exon42:c.6791G>A	p.Arg2264Gln	$9.1x10^{-7}$	26	3	10 (high missense)

Variant nomenclature follows the Human Genome Variation Society (HGVS) recommendations.
Reference sequences used: NM_001110556.2 and NP_001104026.1.
ACMG classification : (3) uncertain significance and (5) pathogenic. * : no match

Table S1: Genetic characteristics and prediction of pathogenicity for both null and missense *FLNA* variants. The frequency of each variant in general populations was determined using GnomAD exome v4. No matches were found for null variants while five missense variants were rarely reported. The variants were classified according to the ACMG (American College of Medical Genetics) guidelines. Different scores were used to predict the pathogenicity of the variants, including the CADD score (Combined Annotation Dependant Depletion) and the MPA score (MoBiDiC Prioritization Algorithm). All null variants were classified as pathogenic (class 5) based on the ACMG guidelines. All missense variants were classified as of “uncertain significance” (class 3).

Supplemental references

1. Lad Y, Kiema T, Jiang P, et al. Structure of three tandem filamin domains reveals auto-inhibition of ligand binding. EMBO J 2007;26(17):3993–4004.

2. Liu J, Lu F, Ithychanda SS, et al. A mechanism of platelet integrin αIIbβ3 outside-in signaling through a novel integrin αIIb subunit–filamin–actin linkage. Blood 2023;141(21):2629–2641.

Supplemental Figures Legends

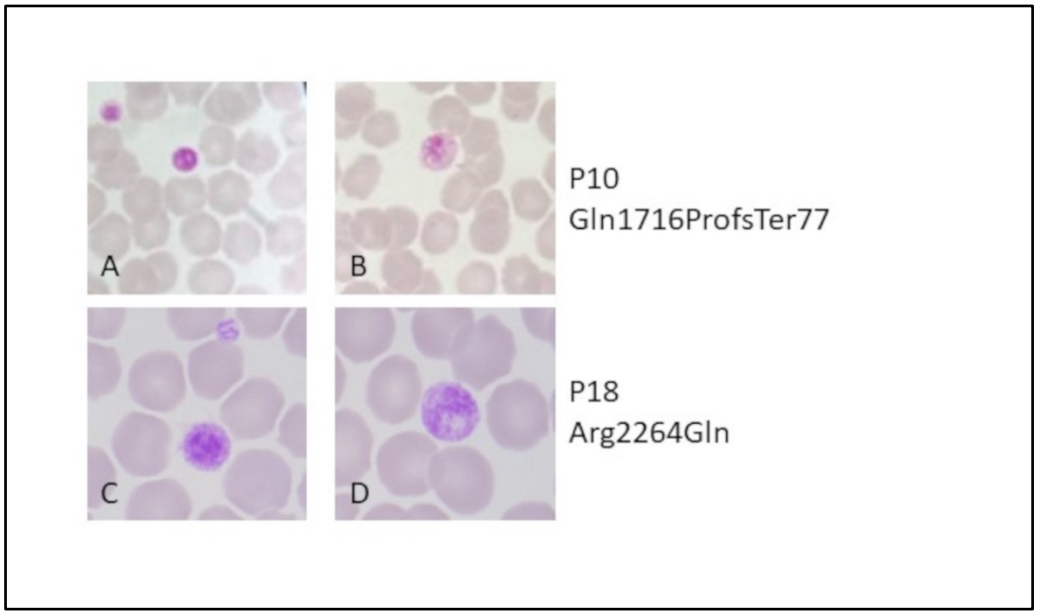

Figure S1 : Platelet morphology evaluated by light microscopy. Smears were stained with May-Grünwald Giemsa. A. and B. show large and giant platelets from P10. C and D. show large and giant platelets from P18.

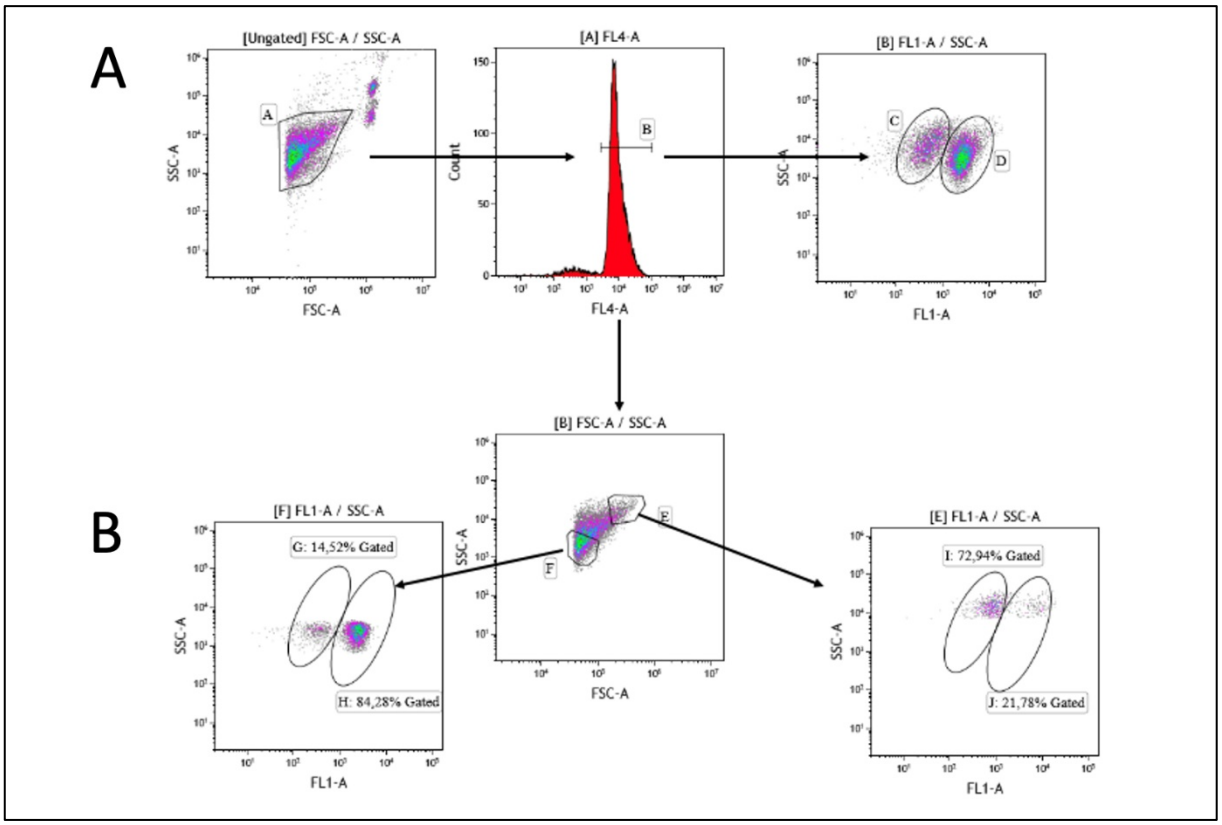

Figure S2: Supplemental files about flow cytometry measurements (FCM). (A) FCM gating strategy. This strategy was used to isolate platelets from fixed blood samples, allowing for the exclusive analysis of the platelet population. First, cells were gated based on their structural and morphological characteristics [first panel, forward scatter/side scatter (FSC/SSC), gate A]. Then, platelets expressing CD41 were selected from gate A (second panel, gate B). The third panel shows two platelet subpopulations isolated from gate B: FLNA-negative platelets (gate C, left) and FLNA-positive platelets (gate D, right). FL4 corresponds to the APC channel, which detects CD41, while FL1 corresponds to the AF488 channel, which detects FLNA. **(B) FLNA-negative platelets are larger than platelet containing FLNA.** Gate E represents the subpopulation of larger platelets in the patient, in which 72% of platelets are FLNA-negative. Gate F focuses on the subpopulation of smaller-sized platelets, which contains 84% FLNA-positive platelets.

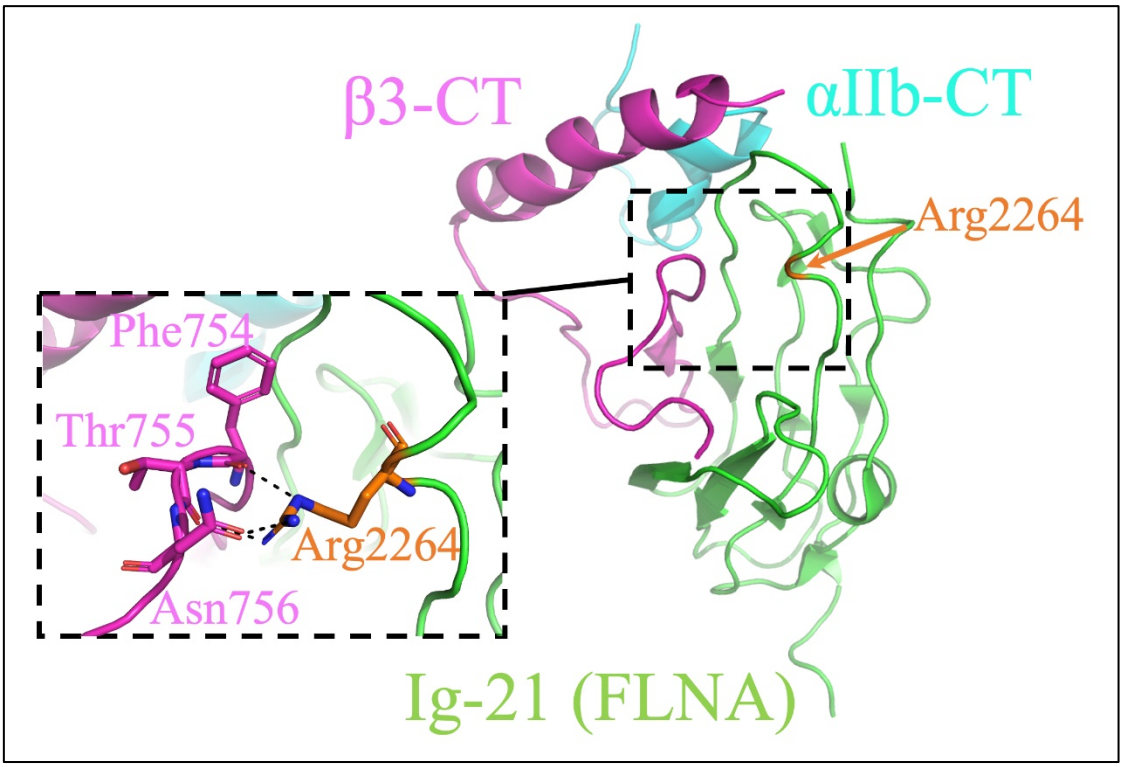

Figure S3: Nuclear magnetic resonance (NMR) structure of the domain 21 of Filamin A (FLNA) in complex with β3-C-terminal (CT) and αIIb-CT peptide (PDB code: 2MTP). The structures of the actin-binding domain and Ig-like domains of the FLNA dimer are known from nuclear magnetic resonance and X-ray crystallography studies.[1] The represented structure was obtained from NMR studies. The ribbon diagram shows the 16th conformer of the Ig-21-αIIbβ3 CT complex with Ig-21 in green and key residue Arg2264 in orange, β3-CT in magenta, and αIIb-CT in cyan. The inset shows a zoom-in of the structure with contact residues Phe754, Thr755, and Asn756 of β3-CT, and Arg2264 of Ig-21. The black dashed lines show 3 hydrogen bonds between contact residues. Arg2264 is involve in transient but strong interaction with integrin αIIbβ3.[2]